

## The effect of Microstructure in Exchange Decoupling of SmCo<sub>5</sub>/Co bi-layers at low temperatures

Rukshan M. Thantirige<sup>1</sup>, Nihar R. Pradhan<sup>2</sup>, Mark T. Tuominen<sup>1</sup>

<sup>1</sup>Department of Physics, University of Massachusetts, 666 N. Pleasant St, Amherst, MA, 01002, USA.

<sup>2</sup>National High Magnetic Field Laboratory, 1800 E. Paul Dirac Drive, Tallahassee, FL-32310, USA.

**Abstract:** Here, we investigated low temperature magnetic properties of SmCo<sub>5</sub>/Co bilayer samples on MgO(100) and glass substrates. Samples were fabricated under identical conditions with a 60 nm Cr underlayer and magnetic properties were measured by a superconducting quantum interference device (SQUID) magnetometer with the maximum applied field of 7 T. Analysis of each layer by an Atomic Force Microscope (AFM) reveals that MgO(100) results in small and uniform SmCo<sub>5</sub> grain formation in contrast to glass. X-ray diffraction studies show that the sample on MgO(100) has high crystallinity with SmCo<sub>5</sub>(11 $\bar{2}$ 0) phase. At room temperature, both samples exhibit good hard magnetic properties with coercivities of 13.2 kOe and 12.5 kOe, deposited on MgO(100) and glass, respectively. Low temperature hysteresis measurements show a development of an exchange decoupling phenomenon below 150 K for the sample on glass, and we propose that this is due to the formation of large magnetic grains on glass that reduces the effective inter-grain exchange coupling between soft and hard magnetic phases.

### I. Introduction

Exchange-coupled magnets that are composites of soft and hard magnetic materials have been explored since its inception by Kneller and Hawig in 1991<sup>1</sup>. This new magnet family has many intriguing properties such as high remanence ( $M_r$ ), high energy products ( $BH$ )<sub>max</sub>, high curie temperatures ( $T_C$ ) and lower cost<sup>1-4</sup>, which made them ideal candidates to replace existing hard magnetic materials for a wide range of applications from data storage to energy efficient appliances. In these magnets, the coercivity ( $H_C$ ) and  $M_r$  are determined by the hard magnetic and the soft magnetic phases, respectively, while effective exchange coupling between the phases holds the key to achieving optimum magnetic properties. This exchange coupling across the soft-hard magnet interface depends not only on materials and their physical dimensions but also on the grain size and distribution of each phase, which made it one of the poorly understood phenomenon in exchange-coupled systems<sup>5</sup>. In addition, in thin films, substrate plays a key role in controlling microstructure which can come as epitaxial guidance, epitaxial mismatch or even de-wetting at given processing conditions, making the microstructure is unique to the substrate<sup>3,6-10</sup>. As a result, samples deposited on different substrates can have very different magnetization reversal paths, producing different magnetic properties even for the same material combination. As an example, Chowdhury *et. al.*<sup>6</sup> reported that SmCo<sub>5</sub>/Co bi-layers grown on MgO(110) and Si(100) under identical processing conditions with same layer thickness resulted energy products of 20.1 MGOe and 12.4 MGOe, respectively.

Here, we studied the reversal of SmCo<sub>5</sub>/Co exchange-coupled bi-layer thin films in the 300-50 K temperature regime, deposited on MgO(100) and glass substrates under identical conditions. We chose MgO(100) and glass as substrates, as previous studies reveal that both these substrates result in high  $H_C$  SmCo<sub>5</sub> thin films<sup>7,8</sup> at room temperature. This study extends beyond the previous work by investigating magnetic properties of SmCo<sub>5</sub>/Co bilayers at temperatures below the room temperature and explored how these properties are affected by the substrate. Room temperature magnetic measurements confirm spring-exchange behavior with high  $H_C$  for both samples, however, low temperature hysteresis measurements show an exchange decoupling like phenomenon for the sample deposited on glass. This transformation from single-step to two-step hysteresis, below a critical temperature, suggests a weakening of exchange coupling.

### II. Sample Preparation

SmCo<sub>5</sub>/Co exchange spring bi-layer films were fabricated in a DC and RF magnetron sputtering system (Orient 8, AJA Inc.) at high vacuum of 10<sup>-8</sup> Torr on MgO(100) (sample A) and glass (sample B) substrates, which were attached to a rotating stage equipped with a heater. Thickness of each layer was fixed at 60 nm, 30 nm and 7.5 nm for the Cr seed layer, SmCo<sub>5</sub> and Co layers, respectively. The nominal thickness of SmCo<sub>5</sub> and Co was determined based on highest  $H_C$  at room temperature with single-step hysteresis. An alloy target with the proper composition was used to deposit SmCo<sub>5</sub>, and both the seed and SmCo<sub>5</sub> layers were sputter deposited at 500°C that is adequate enough to induce in-plane hard magnetic properties of SmCo<sub>5</sub> layer<sup>11,12</sup>. After the growth of Cr and SmCo<sub>5</sub> layers, samples were allowed to cool for 6 hours before depositing Co layer. This is an important

step to minimize inter-diffusion at the SmCo<sub>5</sub>/Co interface, which can change the composition of the hard phase. A 30 nm Cr layer was deposited onto Co layer to protect magnetic layers from oxidation. To investigate grain formation of Cr and SmCo<sub>5</sub> layers, a set of Cr and Cr/SmCo<sub>5</sub> samples were fabricated on both substrates under identical fabrication conditions as of sample A and B. All layers were sputter deposited at 4 mTorr in Ar environment and low sputtering powers were used to keep low deposition rates that promotes continuous film growth.

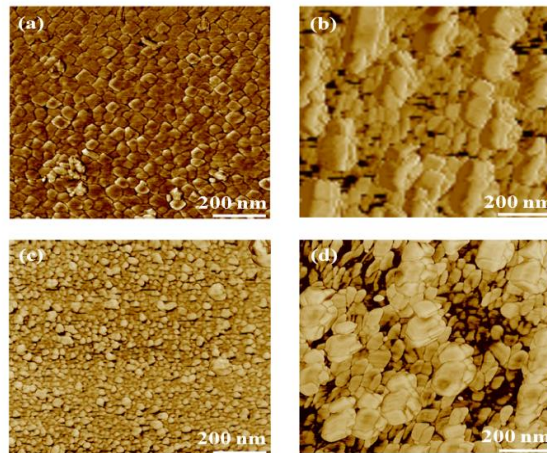


**FIG. 1.** AFM micrograph (phase mode) of Cr (60 nm) underlayer grown at 500 °C on (a) MgO(100) and (b) glass, and SmCo<sub>5</sub>(30 nm) grown at 500 °C on (c) MgO(100) and (d) glass substrates with a 60 nm Cr underlayer.

### III. Results and Discussion

The grain size and distribution of each layer was analyzed by an AFM (Veeco Nanoscope IV, Bruker Inc.) and their crystallinity was investigated by x-ray diffraction with Cu K<sub>α</sub> radiation (X'Pert MRD, Panalytical Inc.). Fig. 1 shows the AFM micrographs of 60 nm Cr underlayer, and 30 nm SmCo<sub>5</sub> hard magnetic layer deposited on Cr underlayer at 500 °C on MgO(100) and glass. As fig. 1(a) and (b) depict, Cr layer deposited on MgO(100) has a nice texture with square shape grains, as opposed to large inhomogeneous Cr grains on glass. This highly textured Cr grain formation might be a result of epitaxial guidance by MgO(100), as reported in previous studies<sup>3, 4</sup>. The average sizes of Cr grains are 26 (± 8) nm and 88 (± 54) nm on MgO(100) and glass, respectively. As shown in fig. 1(c) and (d), SmCo<sub>5</sub> grain formation is unique to the substrate, as Cr/MgO(100) results in smaller SmCo<sub>5</sub> grains with a high degree of uniformity while Cr/glass produces large and inhomogeneous SmCo<sub>5</sub> grains. The average grain sizes are 19 (± 7) nm and 34 (± 32) nm on Cr/MgO(100) and Cr/glass, respectively. These measurements confirm MgO(100) drives small and uniform grain formation in contrast to grains on glass. Previous studies show that small grains and high volume of grain boundaries are crucial for effective interfacial exchange coupling<sup>13, 14</sup>.

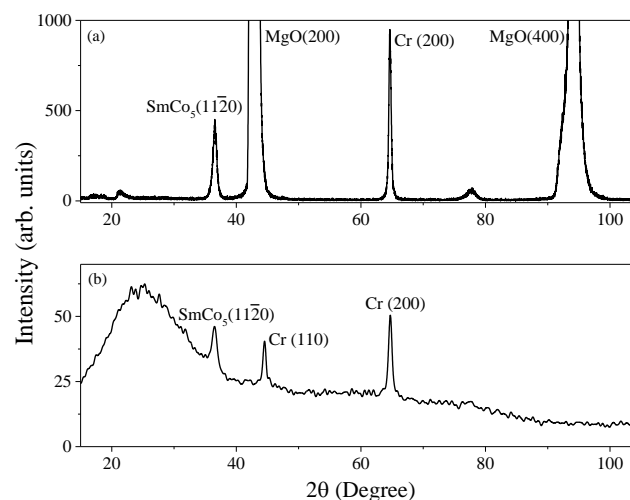


**FIG. 2.** XRD patterns of Co/SmCo<sub>5</sub>/Cr films sputtered onto (a) MgO(100), and (b) glass. The growth temperature was set to 500 °C for SmCo<sub>5</sub> and Cr layers.

Fig. 2 shows x-ray diffraction patterns of sample A(a) and B (b), respectively. For sample A, strong diffraction peaks corresponds to MgO(200), Cr(200) and SmCo<sub>5</sub>(11  $\bar{2}$  0) planes can be observed. The absence of other Cr phases shows that MgO(100) promotes epitaxial growth of Cr(200) that guides the growth of highly textured SmCo<sub>5</sub>(11  $\bar{2}$  0) phase<sup>3,4</sup>. However, the diffraction pattern of sample B shows the presence of both Cr(110) and Cr(200) phases, yet the peak intensity of Cr(110) is roughly one half of the Cr(200) peak. Since Cr(110) is the dominating crystalline phase for isotropic Cr samples grown at room temperature<sup>8, 15</sup>, this strong signal for Cr(200) confirms that the Cr(200) phase is mainly driven by high temperature annealing. The formation of SmCo<sub>5</sub>(11  $\bar{2}$  0) crystals in sample B, guided by Cr(200) phase, shows that in-plane hard magnetic properties are not unrealistic even on amorphous substrates such as glass with a matching buffer layer and proper growth conditions. However, the low intensity of SmCo<sub>5</sub>(11  $\bar{2}$  0) peak assures that most of the SmCo<sub>5</sub> are amorphous. In-plane magnetic properties were measured by a superconducting quantum interference device (SQUID) magnetometer (MPMS-7T, Quantum Design Inc.) with a maximum field of  $\pm 7$  T. Fig. 3 shows normalized hysteresis of both sample A and B measured at 300 K. The  $H_C$  of sample A and B are 13.2 kOe and 12.5 kOe, respectively, suggesting that SmCo<sub>5</sub>(11  $\bar{2}$  0) may be responsible for high  $H_C$  in both samples<sup>16-19</sup>. Although both samples show competitive  $H_C$  values, the sample A has higher  $(BH)_{max}$  of 14.5 MGOe in contrast to 5.3 MGOe of sample B. The low  $(BH)_{max}$  of sample B can be due to low in-plane moment, caused by the random orientation of SmCo<sub>5</sub> grains. This is even reflected in its x-ray diffraction pattern with a weak signal for SmCo<sub>5</sub>(11  $\bar{2}$  0). As a result, high  $H_C$  does not necessarily guarantee a high  $(BH)_{max}$  as random orientation of crystals significantly lowers the effective magnetization and hence the maximum energy product, which is given by<sup>1</sup>,

$$(BH)_{max} = \frac{1}{4} \mu_o M_s^2 \dots\dots\dots (1)$$

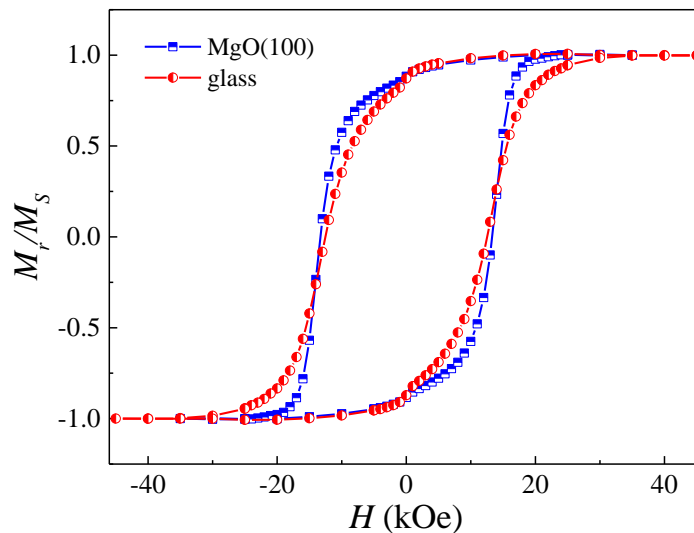
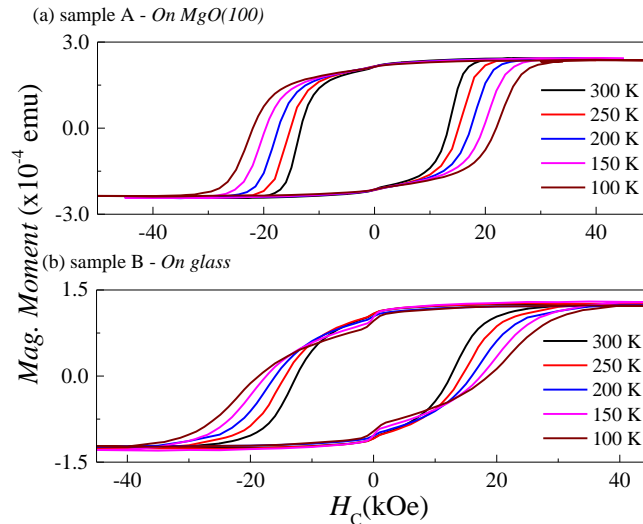


FIG. 3. Normalized room temperature hysteresis curves of SmCo<sub>5</sub>/Co bilayers on MgO(100) and glass substrates grown at 500° C. The sample on MgO(100) shows higher degree of squareness.

The temperature dependent magnetic properties of these two samples were measured from 300 - 50 K and corresponding hysteresis curves for sample A and B are shown in fig. 4(a) and 4(b), respectively. Table 1 depicts the data extracted from fig. 4(a) and 4(b) at various temperatures from 300 K-50 K. For the sample A,  $H_C$  increases linearly from 13.2 kOe at 300 K to 23.3 kOe at 50 K while  $M_S$  largely remains at  $2.42 \times 10^{-4}$  emu for all temperatures, except for a slight drop at 100 K and 50 K (Table 1). The reduce remanence  $M_r/M_S$  fluctuates between 0.88-0.90 with no clear trend with the temperature. It is remarkable to see that at every temperature, the single step hysteresis is preserved. This implies that the exchange coupling between soft and hard phases is preserved at low temperatures. The increase in  $H_C$  can be ascribed to increase in effective magnetocrystalline anisotropy and higher degree of pinning at lower temperatures. However, it can be observed that there is a slight decrease in the squareness of hysteresis loops with lowering the temperature.



**FIG. 4.** Low temperature hysteresis curves measured at 300 K (black), 250 K (red), 200 K (blue), 150 K (magenta), 100 K (brown) for the SmCo<sub>5</sub>/Co sample on (a) MgO(100) and (b) glass. Formation of a ‘shoulder’ can be seen in hysteresis curves in graph (b) for 150 K and 100 K. Note: 50 K hysteresis is not shown for clarity.

For the sample B, the  $H_C$  increases from 12.5 kOe at 300 K to 21.8 kOe at 50 K while the saturation moment shows a random variation with the temperature as shown in Table 1. The reduced remanence  $M_r/M_S$  remains at 0.87-0.88 for 300-200 K temperature regime, however a considerable drop from 0.88 to 0.80 can be seen when reducing the temperature from 200 K to 150 K. This drop in  $M_r/M_S$  coincides with the formation of a ‘shoulder’ in 150 K, 100 K and 50 K (50 K measurement is not shown in fig. 4) hysteresis curves. This transformation from single-step to two-step hysteresis indicates a decoupling of soft and hard phases below a critical temperature. This phenomenon has been previously observed and accounted for exchange decoupling that takes place when lowering the temperature<sup>20, 21</sup> as follows. Based on first principle calculations, effective exchange coupling between soft and hard phases and the single-step reversal require the soft phase to be confined to the size of domain wall width of the hard phase ( $\delta_K$ )<sup>1-3</sup>. However,  $\delta_K$  is governed by the effective anisotropy  $K$ , as  $\delta_K \propto 1/\sqrt{K}$ , which increases with decreasing the temperature. This makes  $\delta_K$  drops when decreasing the temperature, mandating a smaller soft region to keep the exchange coupling intact at lower temperatures. Since the physical size of the soft region remains unchanged, decreasing the temperature makes these two phases partially or fully decoupled, resulting in a two-step hysteresis. However, here, we only see such decoupling for sample B despite both samples having identical soft and hard layer thickness and fabricated under identical conditions. Topographic analysis of these samples (Fig. 1) shows that sample A has small and uniform grains in contrast to sample B, which has large grains and inhomogeneous size distribution. This suggests that exchange decoupling observed for sample B may have been caused by its microstructure. The idea of grain-controlled magnetic properties of thin films can be supported by a number of recent studies that propose smaller grains and uniform distribution favor large inter-grain exchange couplings that enhance the remanence<sup>22-24</sup>. This is in-line with higher remanence and higher  $(BH)_{max}$  of sample A in contrast to that of sample B. Another key observation in hysteresis of sample B is that there is a cross-over between low temperature and high temperature curves (Fig. 4 (b)). This indicates a change of the reversal mechanism due to the exchange decoupling between hard-soft phases that results in a weakening of hard magnetic properties.

**Table 1.** Coercivity ( $H_C$ ), saturation moment and reduced remanence ( $M_r/M_S$ ) for sample A and sample B for temperatures between 300 K – 50 K (extracted from fig. 4)

Temperature (K)	Sample A			Sample B		
	$H_C$ (kOe)	Sat. Moment ( $\times 10^{-4}$ emu)	$M_r/M_S$	$H_C$ (kOe)	Sat. Moment ( $\times 10^{-4}$ emu)	$M_r/M_S$
300	13.2	2.42	0.88	12.5	1.24	0.87
250	15.1	2.41	0.90	14.3	1.26	0.87
200	17.3	2.42	0.89	15.9	1.23	0.88
150	19.6	2.42	0.88	17.4	1.28	0.80
100	22.0	2.38	0.90	18.6	1.23	0.80
50	23.3	2.39	0.89	21.8	1.29	0.79

Fig. 5 shows the variation of the reduced remanence ( $M_r/M_s$ ) and coercivity ( $H_C$ ) with the temperature. As shown in Fig. 5(a),  $H_C$  increases almost linearly with the temperature with slightly different slopes of -0.042 and -0.035 with extrapolated coercivities of 25.76 kOe and 22.84 kOe at 0 K for sample A and B, respectively. This steep increase in  $H_C$  when lowering the temperature for sample A can be associated with large concentration of domain wall boundaries resulted by smaller grains, compared to those of sample B. Further, fig 5(b) shows that  $M_r/M_s$  has no significant temperature dependence for sample A, however, a considerable drop from 0.88 to 0.80 for sample B can be observed when the measuring temperature is reduced from 200 K to 150 K. This could be a result of weakened exchange coupling between soft and hard magnetic grains that essentially reduces the remanence.

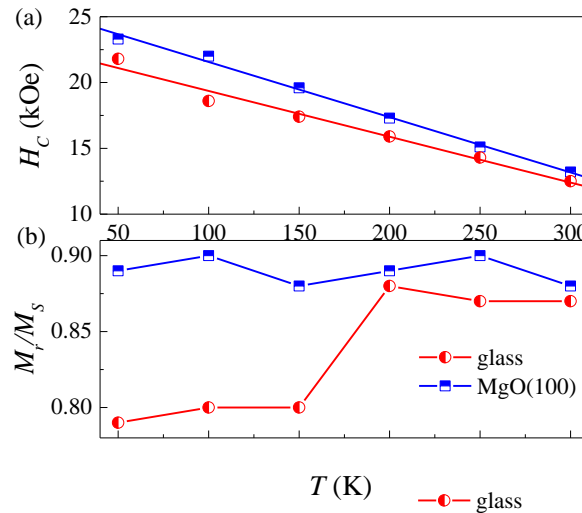


**FIG. 5.** Variation of (a) coercivity ( $H_C$ ), and reduced remanence ( $M_r/M_s$ ) with temperature for sample A (blue) and sample B (red).  $H_C$  was fitted to linear functions with corresponding slopes of -0.042 and -0.035 for sample A and sample B, respectively.

#### IV. Conclusions

In this work, we investigated magnetization reversal of exchange-coupled magnetic thin films fabricated on single crystal MgO(100) and amorphous glass substrates with a 60 nm Cr seed layer. X-ray diffraction studies show that in-plane hard magnetic properties are due to the formation of twisted-crystalline SmCo<sub>5</sub> ( $11\bar{2}0$ ) phase, guided by the Cr (200) seed layer. AFM measurements of each magnetic layer reveals that MgO(100) induced small and uniform grains of 19 ( $\pm 7$ ) nm in contrast to larger grains on glass with a random size distribution, 34 ( $\pm 32$ ) nm. Room temperature hysteresis measurements show that both samples exhibit good hard magnetic properties with high coercivities but  $(BH)_{max}$  of the sample on glass (5.3 MGOe) is almost 1/3 of that of the sample on MgO(100) due to amorphous nature and random orientation of crystals that lowers the effective in-plane magnetization. Hysteresis measurements at lower temperatures reveal an exchange decoupling like phenomenon only for the sample on glass. We believe that this decoupling is induced by the microstructure, as large magnetic grains on glass substrate reduce the effective inter-grain exchange coupling between soft and hard magnetic phases, which is critical against rising anisotropy when lowering the temperature.

#### Acknowledgments

This work was supported by NSF grants DMR-1208042 and NSEC Center for Hierarchical Manufacturing-CMMI-1025020.

#### Reference

- [1]. Kneller, F., Reinhard, H., *Magnetics, IEEE Transactions on* 27.4 (1991): 3588-3560.
- [2]. Skomski, R., Coey, J. M. D., *Physical Review B* 48.21 (1993): 15812.
- [3]. Fullerton, E. E., Jiang, J. S., Bader, S. D., *Journal of Magnetism and Magnetic Materials* 200.1 (1999): 392-404.
- [4]. Fullerton, E. E., Jiang, J. S., Grimsditch, M., Sowers, C. H., Bader, S. D., *Physical Review B*, 58(18), (1998): 12193.
- [5]. Xiao, Q. F., Zhao, T., Zhang, Z. D., Brück, E., Buschow, K. H. J., & de Boer, F. R., *Journal of magnetism and magnetic materials*, 223(3), 215-220, (2001).
- [6]. Chowdhury, P., Krishnan, M., Barshilia, H. C., Rao, D. S., Kumar, D., Shivakumara, C., *Journal of Magnetism and Magnetic Materials*, 342, (2013): 74-79.
- [7]. Zhang, L. N., Hu, J. F., Chen, J. S., Ding, J., *Journal of Applied Physics*, 105(7), (2009): 07A743.
- [8]. Zhang, L. N., Hu, J. F., Chen, J. S., Ding, J., *Journal of Magnetism and Magnetic Materials*, 321(17), (2009): 2643-2647.
- [9]. Zangari, G., Lu, B., Laughlin, D. E., Lambeth, D. N., *Journal of Applied Physics*, 85(8), (1999): 5759-5761.

- [10]. Benaissa, M., Krishnan, K. M., Fullerton, E. E., Jiang, J. S., *IEEE Transactions on Magnetism*, 34(4), (1998): 1204-1206.
- [11]. Saravanan, P., Hsu, J. H., Reddy, G. L. N., Kumar, S., Kamat, S. V., *Journal of Alloys and Compounds*, 574, (2013): 191-195.
- [12]. Malhotra, S. S., Liu, Y., Shan, Z. S., Liou, S., Stafford, D. C., Sellmyer, D. J., *Journal of Applied Physics*, 79(8), (1996): 5958-5960.
- [13]. Verma, K. C., Kotnala, R. K., *Journal of Nanoparticle Research*, 13(10), (2011): 4437-4444.
- [14]. Schrefl, T., Fidler, J., Kronmüller, H., *Physical Review B* 49.9 (1994): 6100.
- [15]. Wyckoff, R. W. G., Crystal structures 1 (7–83). *American Mineralogist Crystal Structure Database*, (1963).
- [16]. Singh, A., Neu, V., Tamm, R., Rao, K.S., Fahler, S., Skrotzki, W., Schultz, L. Holzapfel, B., *Applied Physics Letters*, 87(7), 2005: 072505.
- [17]. Zhang, L. N., Ding, J., Hue, J. F., Chen, J. S., *Nanoelectronics Conference, 2008. INEC 2008. 2nd IEEE International*, 1038-1042.
- [18]. Patra, A. K., Neu, V., Fähler, S., Wendrock, H., Schultz, L., *Journal of applied physics*, 100(4), (2006): 043905.
- [19]. Zhang, J., Song, J. Z., Zhang, Y., Wang, F., Chen, B. C., Shen, B. G., Sun, J. R., *IEEE Transactions on Magnetism*, 47(10), (2011): 2792-2795.
- [20]. Goll, D., Seeger, M., Kronmüller, H., *Journal of Magnetism and Magnetic Materials*, 185(1), (1998): 49-60.
- [21]. Shao, Y. Z., Zhong, W. R., Lan, T., Lee, R. H., *International Journal of Modern Physics B*, 20(01), (2006): 61-72.
- [22]. Herzer, G., *Magnetism, IEEE Transactions on* 26.5 (1990): 1397-1402.
- [23]. Fischer, R., Schrefl, T., Kronmüller, H., Fidler, J., *Journal of Magnetism and Magnetic Materials*, 153(1), (1996): 35-49.
- [24]. Kronmüller, H., Fischer, R., Seeger, M., Zern, A., *Journal of Physics D: Applied Physics*, 29(9), (1996): 2274.